J|A|C|S ARTICLES

Published on Web 04/22/2010

An Adsorption-Based Model for Pulse Duration in Resistive-Pulse Protein Sensing

Lindsay T. Sexton,[†] Hitomi Mukaibo,[†] Parag Katira,[‡] Henry Hess,[‡,§] Stefanie A. Sherrill,[||] Lloyd P. Horne,[†] and Charles R. Martin*[,†]

Department of Chemistry and Center for Research at the Bio/Nano Interface, University of Florida, Gainesville, Florida 32611-7200, Department of Materials Science and Engineering, University of Florida, Gainesville, Florida 32611-6400, Department of Biomedical Engineering, Columbia University, New York, New York 10027, and Department of Chemistry, University of Maryland, College Park, Maryland 20742

Received January 26, 2010; E-mail: crmartin@chem.ufl.edu

Abstract: We have been investigating an electrochemical single-molecule counting experiment called nanopore resistive-pulse sensing. The sensor element is a conically shaped gold nanotube embedded in a thin polymeric membrane. We have been especially interested in counting protein molecules using these nanotube sensors. This is accomplished by placing the nanotube membrane between two electrolyte solutions, applying a transmembrane potential difference, and measuring the resulting ionic current flowing through the nanopore. In simplest terms, when a protein molecule enters and translocates the nanopore, it transiently blocks the ion current, resulting in a downward current pulse. We have found that the duration of such current-pulses are many orders of magnitude longer than the electrophoretic transport time of the protein through the nanotube detection zone. We develop here a simple model that accounts for this key, and previously explained, observation. This model assumes that the protein molecule engages in repeated adsorption/desorption events to/from the nanotube walls as it translocates through the detection zone. This model not only accounts for the long pulse duration but also for the triangular shape of the current pulse and the increase in the standard deviation of the pulse duration with increasing protein size. Furthermore, the results of our analyses are in general agreement with results obtained from other investigations of protein adsorption to surfaces. This includes the observations that smaller proteins stick more readily to the surface but remain adsorbed for shorter times than larger proteins. In addition, the sticking probabilities calculated from our data are in general agreement with results obtained from other methods.

Introduction

There is increasing interest in an electrochemical single-molecule counting experiment called nanopore resistive-pulse sensing.[1−56] In this experiment, a membrane containing a synthetic[1−33] or biological[34−56] nanopore is placed between two electrolyte solutions, a transmembrane potential difference is applied, and the resulting ionic current flowing through the nanopore is measured. The analyte species could be a small molecule,[23] a single-stranded[24] or double-stranded DNA,[25] or

[†] Department of Chemistry and Center for Research at the Bio/Nano Interface, University of Florida.
[‡] Department of Materials Science and Engineering, University of Florida.
[§] Department of Biomedical Engineering, Columbia University.
[||] Department of Chemistry, University of Maryland.

(1) Li, J.; Gershow, M.; Stein, D.; Brandin, E.; Golovchenko, J. A. *Nat. Mater.* **2003**, *2*, 611–615.
(2) Li, J.; Stein, D.; McMullan, C.; Branton, D.; Aziz, M. J.; Golovchenko, J. A. *Nature* **2001**, *412*, 166–169.
(3) Fologea, D.; Gershow, M.; Ledden, B.; McNabb, D. S.; Golovchenko, J. A.; Li, J. *Nano Lett.* **2005**, *5*, 1905–1909.
(4) Chen, P.; Gu, J.; Brandin, E.; Kim, Y.-R.; Wang, Q.; Branton, D. *Nano Lett.* **2004**, *4*, 2293–2298.
(5) Chen, P.; Mitsui, T.; Farmer, D. B.; Golovchenko, J.; Gordon, R. G.; Branton, D. *Nano Lett.* **2004**, *4*, 1333–1337.
(6) Storm, A. J.; Chen, J. H.; Ling, X. S.; Zandbergen, H. W.; Dekker, C. *Nat. Mater.* **2003**, *2*, 537–540.
(7) Storm, A. J.; Storm, C.; Chen, J.; Zandbergen, H.; Joanny, J.-F.; Dekker, C. *Nano Lett.* **2005**, *5*, 1193–1197.
(8) Chang, H.; Kosari, F.; Andreadakis, G.; Alam, M. A.; Vasmatzis, G.; Bashir, R. *Nano Lett.* **2004**, *4*, 1551–1556.
(9) Iqbal, S. M.; Akin, D.; Bashir, R. *Nat. Nanotechnol.* **2007**, *2*, 243–248.
(10) Han, A.; Creus, M.; Schuermann, G.; Linder, V.; Ward, T. R.; de Rooij, N. F.; Staufer, U. *Anal. Chem.* **2008**, *80*, 4651–4658.
(11) Han, A.; Schurmann, G.; Mondin, G.; Bitterli, R. A.; Hegelbach, N. G.; de Rooij, N. F.; Staufer, U. *Appl. Phys. Lett.* **2006**, *88*, 093901/093901–093901/093903.
(12) Carbonaro, A.; Sohn, L. L. *Lab Chip* **2005**, *5*, 1155–1160.
(13) Saleh, O. A.; Sohn, L. L. *Proc. Natl. Acad. Sci. U.S.A.* **2003**, *100*, 820–824.
(14) Saleh, O. A.; Sohn, L. L. *Nano Lett.* **2003**, *3*, 37–38.
(15) Saleh, O. A.; Sohn, L. L. *Rev. Sci. Instrum.* **2001**, *72*, 4449–4451.
(16) Ito, T.; Sun, L.; Crooks, R. M. *Chem. Commun.* **2003**, *7*, 1482–1483.
(17) Ito, T.; Sun, L.; Crooks, R. M. *Anal. Chem.* **2003**, *75*, 2399–2406.
(18) Ito, T.; Sun, L.; Henriquez, R. R.; Crooks, R. M. *Acc. Chem. Res.* **2004**, *37*, 937–945.
(19) Uram, J. D.; Ke, K.; Hunt, A. J.; Mayer, M. *Small* **2006**, *2*, 967–972.
(20) Uram, J. D.; Ke, K.; Hunt, A. J.; Mayer, M. *Angew. Chem., Int. Ed.* **2006**, *45*, 2281–2285.
(21) Uram, J. D.; Mayer, M. *Biosens. Bioelectron.* **2007**, *22*, 1556–1560.
(22) Park, S. R.; Peng, H.; Ling, X. S. *Small* **2007**, *3*, 116–119.
(23) Heins, E. A.; Siwy, Z. S.; Baker, L. A.; Martin, C. R. *Nano Lett.* **2005**, *5*, 1824–1829.
(24) Harrell, C. C.; Choi, Y.; Horne, L. P.; Baker, L. A.; Siwy, Z. S.; Martin, C. R. *Langmuir* **2006**, *22*, 10837–10843.

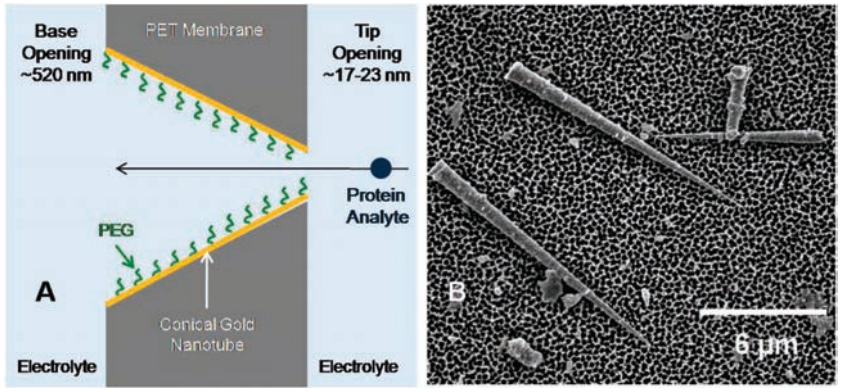

Figure 1. (A) Schematic of the PEG-functionalized conical gold nanotube sensor element showing the base-opening and tip-opening diameters used in these studies. Not to scale. (B) Electron micrograph of such sensor elements after removal from the PET membrane. Note that in the sensing experiment, the nanotube is left embedded in the PET membrane, but it was removed here so that it could be imaged.

a protein or protein complex.[27] In simplest terms, when the analyte enters and translocates the nanopore, it transiently blocks the ion current, resulting in a downward current pulse. In this way, single-molecule pore-translocation events are counted as individual current pulses. The frequency of these current-pulse events is proportional to the concentration of the analyte, and the identity of the analyte is encoded in the current-pulse signature, as defined by the average magnitude and the duration of the current pulses.[30−33]

While deceptively simple, there is much we currently do not understand about this experiment. For example, while downward current pulses are typically obtained, in some cases upward current-pulse events are observed.[8,57,58] In addition, while current pulse durations in the 10s of millisecond range or shorter are most often observed, there are examples of current pulses that last in excess of a second. Such was the case in our recent study of a protein and its antibody complexes using a conical nanotube sensor.[27] Pulses for the free protein, bovine serum albumin (BSA), had an average duration of 0.5 s, and when the antibody anti-BSA was added, the pulse length increased to greater than 2 s. We also found that the average pulse duration scaled with the size of the protein−antibody complex and that the standard deviation of the average also increased with complex size.

As we will show here, such very long-duration pulses cannot be explained in terms of a transport time associated with diffusional or electrophoretic transport of the protein through the nanotube sensing element. Some other factor is determining the magnitude of the pulse duration in this experiment, and in order to probe what this factor might be, we have conducted resistive-pulse experiments on a number of different proteins of differing size and charge. As before, the sensor element was a poly(ethylene glycol)(PEG)-functionalized[59,60] conical gold nanotube[28] prepared by the track-etch method[61−63] in a poly(ethylene terephthalate) (PET) membrane (Figure 1). Again, we observed current pulses with average durations in excess of 1 s and with standard deviations that increase with the size of the protein. We have proposed a simple model that accounts for these key observations. This model assumes that the protein molecule engages in repeated adsorption/desorption events to/from the nanotube wall as it translocates through the detection zone[24,64] in the tip of the nanotube sensor.

This model not only accounts for the long pulse duration but also for the triangular shape of the current pulse and the increase in the standard deviation of the pulse duration with increasing protein size. Furthermore, the results of our analyses are in general agreement with results obtained from other investigations of protein adsorption to surfaces.[65−70] This includes the observations that smaller proteins stick more readily to the surface but remain adsorbed for shorter times than larger

(25) Kececi, K.; Sexton, L. T.; Buyukserin, F.; Martin, C. R. *Nanomed.* **2008**, *3*, 787–796.
(26) Mara, A.; Siwy, Z.; Trautmann, C.; Wan, J.; Kamme, F. *Nano Lett.* **2004**, *4*, 497–501.
(27) Sexton, L. T.; Horne, L. P.; Sherrill, S. A.; Bishop, G. W.; Baker, L. A.; Martin, C. R. *J. Am. Chem. Soc.* **2007**, *129*, 13144–13152.
(28) Siwy, Z.; Trofin, L.; Kohli, P.; Baker, L. A.; Trautmann, C.; Martin, C. R. *J. Am. Chem. Soc.* **2005**, *127*, 5000–5001.
(29) Wang, J.; Martin, C. R. *Nanomed.* **2008**, *3*, 13–20.
(30) Bayley, H.; Martin, C. R. *Chem. Rev.* **2000**, *100*, 2575–2594.
(31) Sexton, L. T.; Horne, L. P.; Martin, C. R. *Mol. BioSyst.* **2007**, *3*, 667–685.
(32) Choi, Y.; Baker, L. A.; Hillebrenner, H.; Martin, C. R. *Phys. Chem. Chem. Phys.* **2006**, *8*, 4976–4988.
(33) Henriquez, R. R.; Ito, T.; Sun, L.; Crooks, R. M. *Analyst* **2004**, *129*, 478–482.
(34) Bayley, H.; Cremer, P. S. *Nature* **2001**, *413*, 226–230.
(35) Howorka, S.; Cheley, S.; Bayley, H. *Nat. Biotechnol.* **2001**, *19*, 636–639.
(36) Kang, X.-F.; Cheley, S.; Guan, X.; Bayley, H. *J. Am. Chem. Soc.* **2006**, *128*, 10684–10685.
(37) Astier, Y.; Braha, O.; Bayley, H. *J. Am. Chem. Soc.* **2006**, *128*, 1705–1710.
(38) Guan, X.; Gu, L.-Q.; Cheley, S.; Braha, O.; Bayley, H. *ChemBioChem* **2005**, *6*, 1875–1881.
(39) Braha, O.; Gu, L.-Q.; Zhou, L.; Lu, X.; Cheley, S.; Bayley, H. *Nat. Biotechnol.* **2000**, *18*, 1005–1007.
(40) Kasianowicz, J. J.; Burden, D. L.; Han, L. C.; Cheley, S.; Bayley, H. *Biophys. J.* **1999**, *76*, 837–845.
(41) Cheley, S.; Gu, L.-Q.; Bayley, H. *Chem. Biol.* **2002**, *9*, 829–838.
(42) Gu, L.-Q.; Braha, O.; Conlan, S.; Cheley, S.; Bayley, H. *Nature* **1999**, *398*, 686–690.
(43) Howorka, S.; Nam, J.; Bayley, H.; Kahne, D. *Angew. Chem., Int. Ed.* **2004**, *43*, 842–846.
(44) Movileanu, L.; Howorka, S.; Braha, O.; Bayley, H. *Nat. Biotechnol.* **2000**, *18*, 1091–1095.
(45) Bezrukov, S. M.; Vodyanoy, I.; Brutyan, R. A.; Kasianowicz, J. J. *Macromolecules* **1996**, *29*, 8517–8522.
(46) Kasianowicz, J. J.; Bezrukov, S. M. *Biophys. J.* **1995**, *69*, 94–105.
(47) Kasianowicz, J. J.; Henrickson, S. E.; Weetall, H. H.; Robertson, B. *Anal. Chem.* **2001**, *73*, 2268–2272.
(48) Halverson, K. M.; Panchal, R. G.; Nguyen, T. L.; Gussio, R.; Little, S. F.; Misakian, M.; Bavari, S.; Kasianowicz, J. J. *J. Biol. Chem.* **2005**, *280*, 34056–34062.
(49) Henrickson, S. E.; Misakian, M.; Robertson, B.; Kasianowicz, J. J. *Phys. Rev. Lett.* **2000**, *85*, 3057–3060.
(50) Kasianowicz, J. J.; Brandin, E.; Branton, D.; Deamer, D. *Proc. Natl. Acad. Sci. U.S.A.* **1996**, *93*, 13770–13773.
(51) Meller, A.; Branton, D. *Electrophoresis* **2002**, *23*, 2583–2591.
(52) Meller, A.; Nivon, L.; Brandin, E.; Golovchenko, J.; Branton, D. *Proc. Natl. Acad. Sci. U.S.A.* **2000**, *97*, 1079–1084.

proteins.[65−69] In addition, the sticking probabilities calculated from our data are in general agreement with results obtained from other methods.[70] We report the results of these investigations here.

Experimental Section

Materials. Bovine serum albumin (BSA, MW 66 kDa), phosphorylase B (MW 97.4 kDa), and β-galactosidase (MW 116 kDa) were obtained from Sigma Aldrich. Poly(ethylene terephthalate) (PET) membranes, 12 μm thick, which contained a single heavy-ion induced damage track, were obtained from GSI (Darmstadt, Germany). A thiolated poly(ethylene glycol) (PEG-thiol, MW 5 kDa) was obtained from Nektar (Huntsville, AL). All other chemicals were of reagent grade and used as received. Purified water (obtained by passing house-distilled water through a Barnstead, E-pure water purification system) was used to prepare all solutions.

Pore Etching and Nanotube Preparation. The same cell was used for etching, electrochemical determination of the dimensions of the pore, and resistive-pulse experiments.[62] It is a two-compartment Kel-F cell in which the PET membrane separates the two half-cells. The damage track in the PET membrane was chemically etched into a conically shaped pore using the two-step etching method described in detail previously.[62] Conically shaped nanopores and tubes have two openings, the large-diameter (or base) opening at one face of the membrane and the small-diameter (or tip) opening at the opposite face (Figure 1A). We have shown that the two-step etching method provides for excellent reproducibility in both the tip and the base diameters.[62] Pores with base diameters of 520 nm, as determined by electron microscopy,[62] were used.

The diameter of the tip opening was determined using an electrochemical method[61] described in detail in our prior work.[23,24] Briefly, the membrane containing the single conical nanopore was mounted in the cell, and an electrolyte solution of measured conductivity was placed on either side of the membrane. For these studies, this solution was 1 M KCl, pH 6, with a measured conductivity of 10 S/m. A current−voltage curve was obtained, the slope of which is the ionic conductance of the electrolyte-filled nanopore. The conductance is used to calculate the diameter of the tip opening.[23,24,61] The nanopores used for these studies had tip diameters before deposition of the gold nanotube (vide infra) of 50 nm.

The electroless-plating method described previously was used to deposit the conically shaped gold nanotube (Figure 1) within the pore.[71] Electroless plating also yields gold surface films covering both faces of the membrane. Our prior work showed that these gold surface films cause an unwanted double-layer charging component to the current−voltage curve for that nanotube membrane.[27] For this reason, the gold surface films were removed by scrubbing with an ethanol-wetted cotton swab. A current−voltage curve obtained after plating was used to provide the diameter of the tip opening of the resulting gold nanotube. The diameter of the much larger base opening remained essentially unchanged after plating.

PEG-thiol was then attached to the gold surfaces to suppress nonspecific protein adsorption.[27,59,60] However, as was reported in our prior study,[27] and as will be elaborated on here, protein adsorption cannot be completely eliminated. The nanotube membrane was immersed into a 0.1 mM solution of the PEG-thiol in purified water at 4 °C for ∼15 h. The membrane was then rinsed in purified water, and the diameter of the tip opening was remeasured. The tip diameters reported here are the diameters measured after PEG functionalization. Nanotubes with tip diameters of 17 and 23 nm were used for these studies.

Current-Pulse Measurements. The membrane sample containing the PEG-functionalized conical gold nanotube was mounted in the cell, and both half cells were filled with ∼3.5 mL of 10 mM phosphate buffer solution (pH = 7.4) that was also 100 mM in KCl. A Ag/AgCl electrode (BAS, West Lafayette, IN) was placed into each half-cell solution and connected to an Axopatch 200B (Molecular Devices Corporation, Union City, CA) patch-clamp amplifier. The Axopatch was used to apply the desired transmembrane potential and measure the resulting ion current flowing through the electrolyte-filled nanotube. The current was recorded in the voltage-clamp mode with a low-pass Bessel filter at 2 kHz bandwidth. The signal was digitized using a Digidata 1233A analog-to-digital converter (Molecular Devices Corp.) at a sampling frequency of 10 kHz. Data were recorded and analyzed using pClamp 9.0 software (Molecular Devices Corp.).

Unless otherwise stated, the applied transmembrane potential was 1 V with polarity such that the Ag/AgCl anode was in the half-cell solution facing the base opening and the Ag/AgCl cathode in the solution facing the tip opening. Because the p*I* values of BSA, phosphorylase B, and β-galactosidase are ∼4.8,[72] 5.8−6.3,[73,74] and ∼4.6,[75] respectively, all the proteins have net negative charge in the pH = 7.4 buffer used here. All proteins were added to the half-cell solution facing the tip opening and driven electrophoretically through the nanotube sensor from tip to base (Figure 1).

Results and Discussion

Steady-State Current and Current-Pulse Events for BSA, Phosphorylase B, and β-Galactosidase. In the absence of protein analyte, a steady-state ion current (no current-pulse events) of ∼820 pA was observed for the PEG-functionalized nanotube with tip diameter of 17 nm (Figure 2A). As discussed previously,[23,24,27,64] conical nanopores and nanotubes have an analyte-detection zone just inside the tip opening. When a solution 100 nM in BSA was added to the half-cell facing the tip opening, current-pulses associated with the electrophoretic transport of BSA through the detection zone were observed (Figure 2B). After sensing BSA, the nanotube sensor was thoroughly rinsed and the steady-state ion current (no current-pulse events) returned (Figure 2C). Solutions 100 nM in phosphorylase B (PhB) and β-galactosidase (βGal) were subsequently sensed with the same nanotube sensor (Figure 2D,E).

(53) Meller, A.; Nivon, L.; Branton, D. *Phys. Rev. Lett.* **2001**, *86*, 3435–3438.
(54) Deamer, D. W.; Branton, D. *Acc. Chem. Res.* **2002**, *35*, 817–825.
(55) Bezrukov, S. M.; Kullman, L.; Winterhalter, M. *FEBS Lett.* **2000**, *476*, 224–228.
(56) Kullman, L.; Winterhalter, M.; Bezrukov, S. M. *Biophys. J.* **2002**, *82*, 803–812.
(57) Zhe, J.; Jagtiani, A.; Dutta, P.; Hu, J.; Carletta, J. *J. Micromech. Microeng.* **2007**, *17*, 304–313.
(58) Smeets, R. M. M.; Keyser, U. F.; Krapf, D.; Wu, M.-Y.; Dekker, N. H.; Dekker, C. *Nano Lett.* **2006**, *6*, 89–95.
(59) Yu, S.; Lee, S. B.; Martin, C. R. *Anal. Chem.* **2003**, *75*, 1239–1244.
(60) Yu, S.; Lee, S. B.; Kang, M.; Martin, C. R. *Nano Lett.* **2001**, *1*, 495–498.
(61) Apel, P. Y.; Korchev, Y. E.; Siwy, Z.; Spohr, R.; Yoshida, M. *Nucl. Instrum. Methods Phys. Res., Sect. B* **2001**, *184*, 337–346.
(62) Wharton, J. E.; Jin, P.; Sexton, L. T.; Horne, L. P.; Sherrill, S. A.; Mino, W. K.; Martin, C. R. *Small* **2007**, *3*, 1424–1430.
(63) Apel, P. *Nucl. Instrum. Methods Phys. Res., Sect. B* **2003**, *208*, 11–20.
(64) Lee, S.; Zhang, Y.; White, H. S.; Harrell, C. C.; Martin, C. R. *Anal. Chem.* **2004**, *76*, 6108–6115.
(65) MacRitchie, F. *J. Colloid Interface Sci.* **1985**, *105*, 119–123.
(66) Fainerman, V. B.; Leser, M. E.; Michel, M.; Lucassen-Reynders, E. H.; Miller, R. *J. Phys. Chem. B* **2005**, *109*, 9672–9677.
(67) Jeon, S. I.; Andrade, J. D. *J. Colloid Interface Sci.* **1991**, *142*, 159–166.
(68) Lobel, K. D.; Hench, L. L. *J. Sol-Gel Sci. Technol.* **1996**, *7*, 69–76.
(69) Katira, P.; Agarwal, A.; Hess, H. *Adv. Mater.* **2009**, *21*, 1599–1604.
(70) Weaver, D. R.; Pitt, W. G. *Biomaterials* **1992**, *13*, 577–584.
(71) Menon, V. P.; Martin, C. R. *Anal. Chem.* **1995**, *67*, 1920–1928.
(72) Peng, Z. G.; Hidajat, K.; Uddin, M. S. *J. Colloid Interface Sci.* **2005**, *281*, 11–17.
(73) Green, A. A. *J. Biol. Chem.* **1945**, *158*, 315–319.
(74) Bo, T.; Pawliszyn, J. *Anal. Chim. Acta* **2006**, *559*, 1–8.

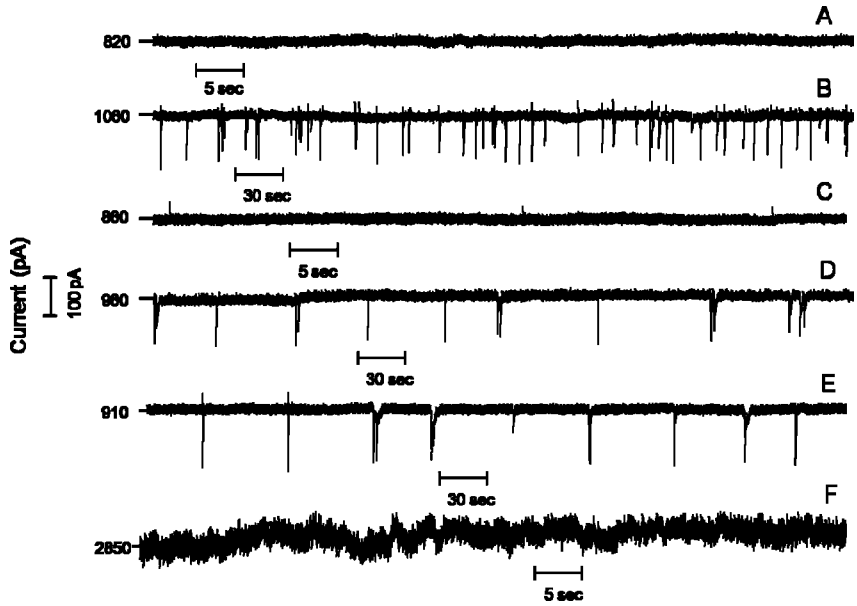

Figure 2. Current−time transients for a PEG-functionalized conical nanotube sensor with tip diameter = 17 nm: (A) buffer only; (B) buffer plus 100 nM BSA; (C) buffer only after sensing 100 nM BSA; (D) buffer plus 100 nM PhB; (E) buffer plus 100 nM βGal (applied transmembrane potential for A−E was 1000 mV); (F) buffer plus 100 nM BSA at an applied transmembrane potential of −1000 mV.

After further rinsing, these current-pulse events ceased and the steady-state current with no events was restored. That these current pulses are due to electrophoretic transport is supported by the fact that when the polarity is reversed, no current pulses are observed (Figure 2F). This is because, with this polarity, the protein molecules are driven electrophoretically away from the nanotube membrane. As will be discussed below, the steady-state current is higher (~2850 pA) at reversed polarity (Figure 2F vs Figure 2A) because after exposure to the proteins the nanotube acts as an ion current rectifier.[76−78]

Close inspection of the current−time transients in Figure 2 reveals that the steady-state current (between pulses) in the presence of 100 nM BSA (~1060 pA) is higher than the steady current in the absence of BSA (~820 pA). When the BSA solution was removed and replaced with buffer, the baseline current decreased to ~860 pA but never returned to the lower pre-BSA-exposure value. In the presence of 100 nM PhB and 100 nM βGal, the steady-state current again rose to ~960 and ~910 pA, respectively. When these protein solutions were removed and replaced with buffer, the baseline current decreased again to ~860 pA.

The origins of this effect have been described in our prior work.[27] Briefly, the increase in steady-state current is a result of protein molecules adsorbing to portions of the gold nanotube walls that remain exposed under the PEG layer. Protein adsorption introduces excess negative charge on the nanotube walls. This causes the nanotube to function as an ion-current rectifier.[76−78] This ion-current rectification phenomenon results in a large increase in current at negative potentials (Figure 2F) and a slight increase at positive potentials (Figures 2B−E).

An expanded view of a typical current-pulse event for each protein is shown in Figure 3. In all cases, the current pulse drops sharply and then tails upward with time.[27] This shape reflects the fact that the protein is driven into the tip, where it is most effective at blocking the ion current, and driven toward the base, where it becomes less and less effective at blocking the current.[27] The current-pulse events can be characterized by the current-pulse amplitude (Δi) and the current-pulse duration (τ). Δi is defined as the difference in current between the baseline and the lowest current within a pulse, and τ is defined as the time interval between the precipitous drop and the time when the current returns to the baseline value.[27]

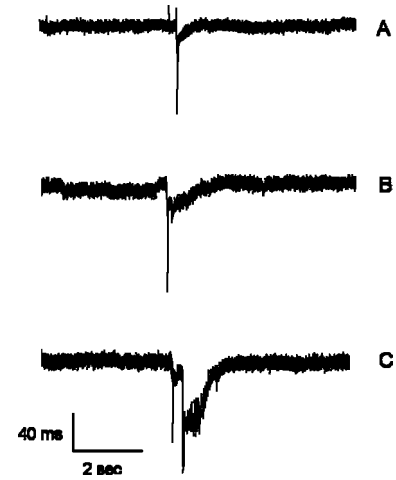

Figure 3. Expanded views of typical current pulses associated with tip-to-base translocation of (A) BSA, (B) PhB, and (C) βGal. 100 nm protein. Tip diameter =17 nm. Transmembrane potential = 1000 mV.

Scatter Plot and Histograms. In order to obtain average values and standard deviations for the current-pulse amplitude and duration, histograms of Δi and τ were plotted for each protein (Figures 4 and 5). The average Δi and τ values and standard deviations were obtained by fitting the histograms to a Gaussian distribution (solid curves).[4,27,37,50−52]

As noted in the Introduction, the key objective of this study was to investigate how protein size affects the current-pulse

(75) Komp, M.; Hess, D. *Z. Pflanzenphysiol.* **1977**, *81*, 248–259.
(76) Siwy, Z.; Heins, E.; Harrell, C. C.; Kohli, P.; Martin, C. R. *J. Am. Chem. Soc.* **2004**, *126*, 10850–10851.
(77) Harrell, C. C.; Kohli, P.; Siwy, Z.; Martin, C. R. *J. Am. Chem. Soc.* **2004**, *126*, 15646–15647.
(78) Heins, E. A.; Baker, L. A.; Siwy, Z. S.; Mota, M. O.; Martin, C. R. *J. Phys. Chem. B* **2005**, *109*, 18400–18407.

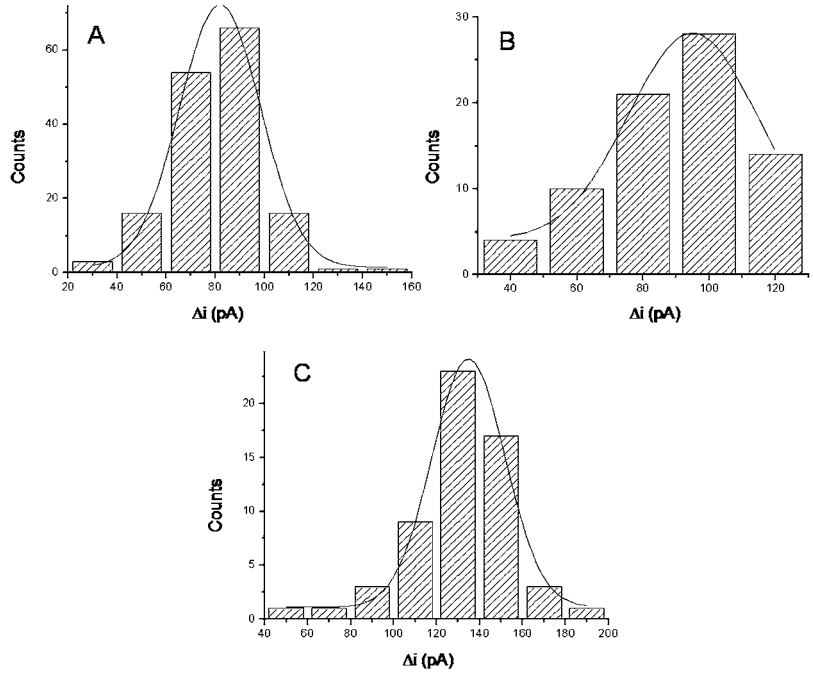

Figure 4. Histograms of current-pulse amplitude data: (A) 100 nM BSA; (B) 100 nM phosphorylase B; (C) 100 nM β-galactosidase. Solid curves are Gaussian fits. Applied transmembrane potential = 1000 mV. Tip diameter = 17 nm.

signature. The hydrodynamic diameter for BSA, calculated from the diffusion coefficient, is 6.8 nm.[79] The hydrodynamic diameters of PhB and βGal are 9.8[80] and 16.6 nm,[81] respectively. Figure 4 shows the Δi histogram for each protein when a nanotube with a tip diameter of 17 nm was used as the sensor. The average Δi values for BSA, PhB, and βGal are 80 $\pm$ 15, 95 $\pm$ 20, and 135 $\pm$ 20 pA, respectively, where the standard deviations values are for the best-fit Gaussian curve for each distribution in Figure 4. These data show that while Δi in general increases with protein size, it would be difficult to distinguish between these three proteins on the basis of the current-pulse amplitude alone.

Figure 5 shows the corresponding current-pulse duration, τ, histogram for each protein, and the average τ values are shown in Table 1. τ, in general, increases with the size of the protein with the largest protein, βGal, giving τ of almost two seconds. Furthermore, as was observed for the BSA/anti-BSA complexes studied previously,[27] the standard deviation of the τ value also increases with the size of the protein molecule. For reasons discussed in our prior work,[27] we have also found that, within experimental error, τ is independent of tip diameter (Table 1).

These trends in the current-pulse amplitude and duration data can be visualized more clearly via scatter plots of Δi vs τ (Figure 6). The large spread in the current-pulse duration data for the largest protein, βGal, is clearly seen, as is the much smaller spread for the smallest protein, BSA. This plot suggests that βGal could be distinguished from BSA because only βGal produces pulses in the upper right quadrant of this plot, and only BSA produces pulses in the lower left quadrant. Distinguishing PhB from the other two proteins based purely on such current-pulse data would be problematic. However, previous reports have shown that protein-analytes can be detected after binding to specific antibodies.[13,20,27] We have shown that protein specificity can be introduced to the pulse duration by adding an antibody that selectively binds to the target protein-analyte in the analyte solution.[27] Hence, one does not have to rely on the current-pulse signature of the protein by itself to determine whether a particular analyte protein is present in the sample.

Table 1. Current-Pulse Duration (τ) Data for the Indicated Proteins and Nanotube Tip Diameters (Protein Concentration 100 nM)

tip diameter (nm)	protein	τ (ms)
17	BSA	520 $\pm$ 110
	PhB	1060 $\pm$ 230
	βGal	1920 $\pm$ 870
23	BSA	440 $\pm$ 160
	PhB	663 $\pm$ 330
	βGal	1200 $\pm$ 570

Modeling the Current-Pulse Duration Data. The τ values obtained with our conical nanotube sensors (Table 1) are much longer than durations typically obtained with other resistive-pulse sensors. For example, τ values for DNA analytes with the biological α-hemolysin sensor are typically less than 20 ms.[37] Furthermore, our prior work with conical nanopore sensors and a large DNA analyte yielded τ values of less than 80 ms.[24] These results are of particular interest because the radius of gyration of the DNA molecule was a factor of 3 times greater than the nanopore tip radius. Nevertheless, the DNA τ value was over an order of magnitude smaller than the τ values observed for the protein analytes studied here. We describe below a simple model that accounts for the very long pulse durations observed for protein analytes.

We begin with the concept of the detection zone[23,24,27,64] in conical nanopore and nanotube resistive-pulse sensors. As discussed above, a protein molecule is most effective at blocking the ion current flowing through the conical nanotube when it is in the tip region, and the molecule becomes less effective at blocking the current as it is driven toward the tube base. Hence, there is an analyte-detection zone in the tip region.[23,24,27,64] In order to

(79) Gaigalas, A. K.; Hubbard, J. B.; McCurley, M.; Woo, S. *J. Phys. Chem.* **1992**, *96*, 2355–2359.
(80) DeVincenzi, D. L.; Hedrick, J. L. *Biochemistry* **1967**, *6*, 3489–3497.
(81) Auersch, A.; Littke, W.; Lang, P.; Burchard, W. *J. Cryst. Growth* **1991**, *110*, 201–207.

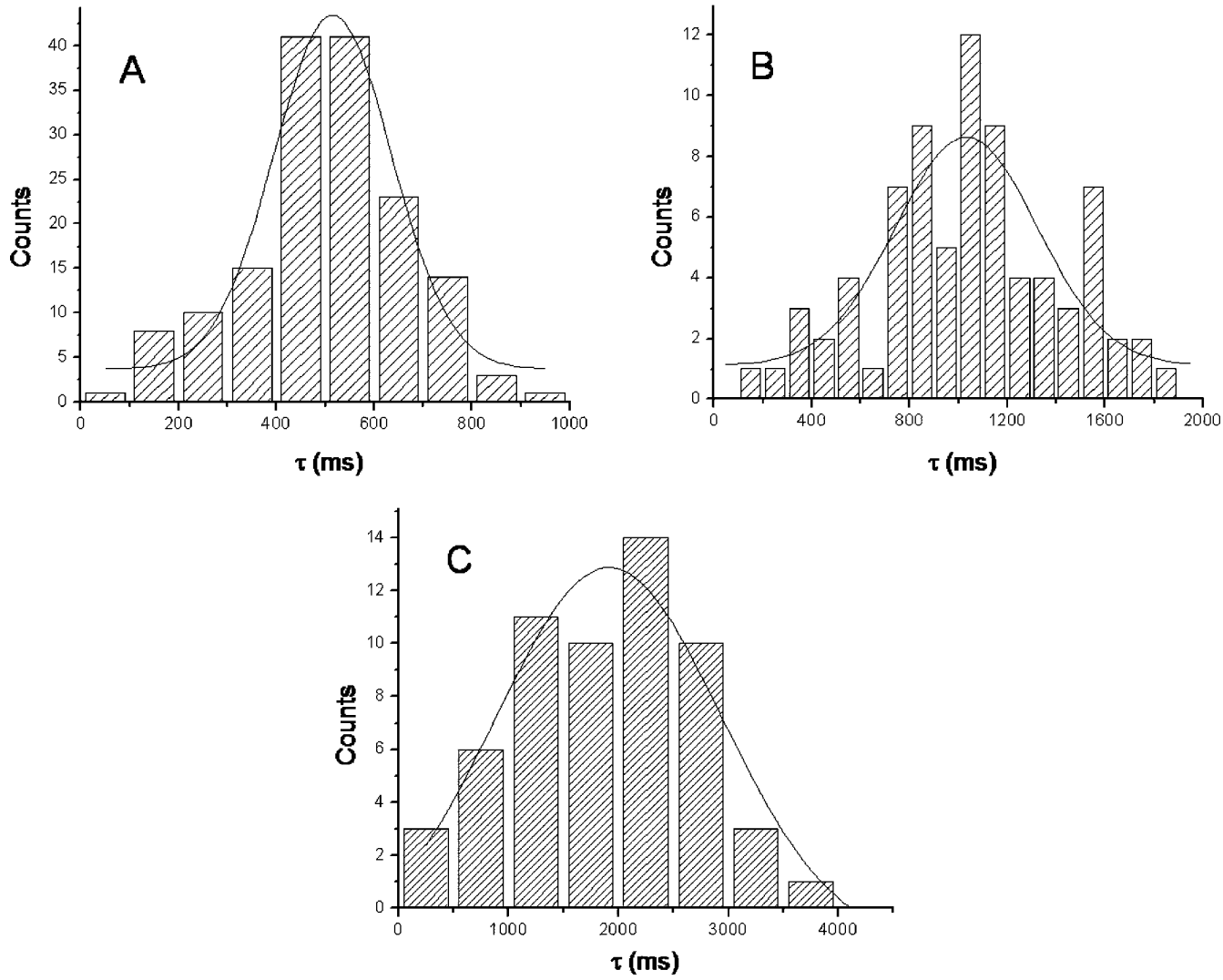

Figure 5. Histograms of current-pulse duration data: (A) 100 nM BSA; (B) 100 nM PhB; (C) 100 nM βGal. Solid curves are Gaussian fits. Applied transmembrane potential = 1000 mV. Tip diameter = 17 nm.

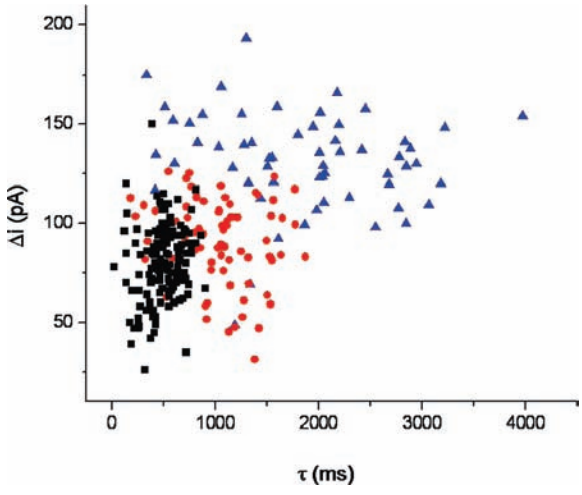

Figure 6. Scatter plot of current-pulse magnitude (Δi) versus current-pulse duration (τ) for 100 nM BSA (black □), 100 nM phosphorylase B (red ●), and 100 nM β-galactosidase (blue ▲). Applied transmembrane potential = 1000 mV. Tip diameter = 17 nm.

understand the long current-pulse durations observed here (Table 1), we need a definition for the length of this detection zone.

The definition we propose here is based on the ratio of the cross-sectional area of the analyte protein (A_p) to the cross-sectional area of the tube, at any point along the tube length, x (A_{tx}). This ratio is at a maximum when the protein just enters the tip of the tube and decreases as the protein is driven toward the base. Ultimately, the ratio A_p/A_{tx} becomes so small that the protein is no longer effective at blocking the ion current. This assertion is confirmed by the characteristic shape of the current pulses observed here (Figure 3). We assume here that when A_p/A_{tx} decreases to 0.01, the protein is no longer effective at blocking the ion current. Hence the detection zone length is that distance, x, from the tip opening where $A_p/A_{tx} = 0.01$. The detection zone lengths calculated based on this definition are shown in Table 2. As would be expected, the detection zone is longer for larger proteins and for sensors with smaller tip diameter.

With the length of the detection zone defined, we can now calculate how long it would take for a protein molecule to be driven by electrophoresis through the detection zone. This calculation[82] requires that the charge on the protein and the field strength in the detection zone are known. The field strength value was taken from finite element simulations described previously.[27] We use BSA to illustrate this calculation here, and assume it has a charge of −20 in the pH = 7.4 buffer used

Table 2. Length of Detection Zone Calculated Based on the Cross-Sectional Area of the Protein Analytes and Conical Pore

			tip diameter = 17 nm (cross-sectional area at tip = 230 nm^2)		tip diameter = 23 nm (cross-sectional area at tip = 420 nm^2)	
protein	hydrodynamic radius (nm)	cross-sectional area of protein (area occupied inside the nanopore) (nm^2)	% blockage at tip	length of detection zone (nm)	% blockage at tip	length of detection zone (nm)
BSA	3.4	36	16	1170	9	1030
PhB	4.9	75	33	1810	18	1670
βGal	8.3	220	96	3460	52	3320

in this work.[83] We obtain an electrophoretic transport time for BSA through the ~1 μm detection zone for the 23-nm-tip sensor (Table 2) of approximately 60 μs. This is almost 4 orders of magnitude smaller than the experimental current-pulse duration for BSA with this sensor (Table 1).

This simple calculation shows that some physical or chemical phenomenon is strongly impeding the electrophoretic transport of the protein though the detection zone. This is also supported by the calculations by Li et al., who found that the diffusion coefficient of BSA within a silicon nitride nanopore was 3 orders of magnitude smaller than the bulk solution value.[84] They concluded that the BSA molecule was strongly confined within the nanopore but did not elaborate on the mechanism of confinement. In the Supporting Information we discuss a number of different processes that might impede protein transport, and attempt to rationalize these processes with the observed current-pulse shape and duration. Based on these analyses, we propose here that protein transport is impeded by multiple adsorption and desorption events of the protein to the nanotube walls during translocation through the detection zone.

The model assumes that the protein enters an energy-well when it collides with and adsorbs to the nanotube wall. In order for the protein to exit this well (desorb), it must overcome an activation barrier, E_A. The rate constant for desorption is given by the Arrhenius equation[85]

$$k = Ae^{-E_A/k_bT} \tag{1}$$

where A is the frequency factor, k_b is the Boltzmann constant, and T is the temperature. If we call the concentration of protein molecules adsorbed on the surface [S], then the desorption of the protein molecules can be described by a first-order reaction equation:[86]

$$-\frac{d[S]}{dt} = k[S] \tag{2}$$

If [T] is the concentration of binding sites on the surface, then the probability that a binding site is filled, P_A, can be expressed as $P_A = [S]/[T]$. Thus, eq 2 can be rewritten as

$$-\frac{d[S]}{[T]dt} = k[S]/[T] \tag{3}$$

or

$$-\frac{dP_A}{dt} = kP_A \tag{4}$$

The probability that the protein molecule initially present has desorbed, P_D, can also be expressed as $dP_A/dt = -dP_D/dt$. Substituting eq 4 for dP_A/dt gives

$$\frac{dP_D}{dt} = kP_A = k(1 - P_D) \tag{5}$$

The right most side of this equation results because $P_D + P_A = 1$. Integration with respect to t yields

$$P_D = 1 - e^{-kt} \tag{6}$$

This can also be written in terms of the probability that the molecules remains adsorbed

$$P_A = e^{-kt} \tag{7}$$

Equation 4 shows that the probability that a protein molecule remains adsorbed to the nanotube decreases exponentially with time. For such a distribution the mean time that a molecule remains adsorbed, $\langle t \rangle$, is $1/k$, and the variance of the distribution is $\langle t \rangle^2$ or $1/k^2$.[87] If we assume that a protein molecule translocating the detection zone engages in N_a adsorption/desorption events, then the experimental current-pulse duration, τ, is given by

$$\tau = N_a\langle t \rangle \tag{8}$$

Likewise, the variance of the experimental current-pulse duration, Var(τ), is given by

$$\mathrm{Var}(\tau) = N_a\langle t \rangle^2 \tag{9}$$

Solving eq 8 for τ, and substituting into eq 9 yields

$$\mathrm{Var}(\tau) = N_a(\tau/N_a)^2 = \tau^2/N_a \tag{10}$$

The standard deviation, σ, of the experimental current-pulse duration is the square root of the variance

$$\sigma = \tau/N_a^{1/2} \tag{11}$$

which can be rearranged to

$$N_a = (\tau/\sigma)^2 \tag{12}$$

The error in the τ values is, of course, propagated through eq 12 to give a standard deviation for the number of adsorption events, N_a. From the rules of propagation of error[88] the percent standard deviation in N_a is twice the percent standard deviation of τ. Since both τ and σ are known experimentally (Table 1), the average number of adsorption/desorption events, N_a, that each protein makes as it translocates the detection zone can be calculated, as can the average duration of a sticking event, $\langle t \rangle$, which is just the pulse duration, τ, divided by N_a (Table 3).

(82) See the Supporting Information for details.
(83) Yu, Y.-X.; Tian, A.-W.; Gao, G.-H. *Phys. Chem. Chem. Phys.* **2005**, *7*, 2423–2428.
(84) Fologea, D.; Ledden, B.; McNabb, D. S.; Li, J. *Appl. Phys. Lett.* **2007**, *91*, 053901/053901–053901/053903.

Table 3. Number and Duration of Protein Sticking Events and the Number of Protein Collisions with the Nanotube Walls and Sticking Probabilities Calculated for Each Protein

tip diameter (nm)	protein	no. of sticking events	duration of sticking events $<t>$ (ms)	no. of collisions	sticking probability ($\times 10^5$)
17	BSA	22	25	42000	50
	PhB	21	50	577000	3.6
	βGal	5	380	257000	2.0
23	BSA	8	55	20000	40
	PhB	4	165	294000	1.4
	βGal	4	300	144000	2.8

Considering the $<t>$ data first, we see that the average time a protein remains adsorbed to the nanotube wall increases with increasing protein size. This indicates that the rate of desorption of the protein from the surface decreases with increasing protein size. Similar results have been obtained in other investigations of protein desorption from surfaces.[65−67] Calculations by Jeon and Andrade, which showed that the van der Waals interaction between a protein and a PEG-coated surface increases with protein size, help explain these observations.[67] In addition, opportunities for other types of interactions, such as dipole−dipole and hydrogen bonding, will, in general, also increase with protein size. As a result of these cumulative attractive forces, the activation energy for desorption of the protein increases with protein size, and this accounts for the decrease in desorption rate constant with protein size.

It is more difficult to directly compare the number of sticking events for the different proteins because the detection zone lengths are different for each protein (Table 2). For example, since the detection zone for βGal is longer than for BSA (Table 2), βGal has more opportunities to collide with the nanotube walls than does BSA. In order to account for these differences, we have calculated the number of collisions that each protein makes with the nanotube walls as it traverses the detection zone, N_c. This calculation takes into account the different sizes of the proteins and the different lengths of the detection zones. This allows us to calculate the sticking probability for each protein to the nanotube wall via $P_s = N_a/N_c$ (Table 3).

In order to calculate N_c we must know the total surface area of the tube walls in the detection zone, A_{tw}; this can be calculated from the cone angle of the tube and the detection zone length.[82] The concentration, C_p, of the protein in the detection zone must also be known. Since we are analyzing single-current pulse events, we assume that there is only one protein molecule in the detection zone during the event. Therefore, C_p, in units of protein molecules per m^3, is simply one molecule divided by the volume of the detection zone. The volume can, again, be calculated from simple geometric arguments.[82] Finally, we need to know the electrophoretic transport time through the detection zone, t_z, which we have already discussed, and the molecular mass of the protein, m_p, in units of kg per molecule.

With these numbers in hand, we can calculate the number of collisions that the protein makes with the tube walls in the detection zone, N_c, via[82]

$$N_c = t_z A_{tw} C_p \sqrt{k_b T / m_p} \quad (13)$$

where k_b is the Boltzmann constant and T is the temperature. The N_c values for the three proteins and two nanotube sensors investigated here are shown in Table 3, as are the sticking probabilities, P_s, calculated with these numbers.

The key conclusion from these calculations is that the sticking probabilty for the smallest protein, BSA, is significantly larger than for the largest protein, βGal. This indicates that the rate of adsorption is higher for the smaller protein. Similar results were obtained by Lobel et al. in a study of the adsorption of various proteins onto sol−gel derived glass.[68] In this work adsorption kinetics of three proteins onto the glass were measured spectroscopically. Like us, they found that the adsorption rate increased as the size of the proteins decreased.

The higher adsorption rate suggests that the activation energy for adsorption is lower for small proteins. This can be explained by considering the steric repulsion between the PEG surface and the protein.[89] Steric repulsion has two terms. The first concerns the compression of the PEG chains as the protein approaches the surface. Compression lowers the entropy of the PEG chains, and this acts as a repulsive effect. The second term concerns the loss of hydration of the polymer chains when they are compressed by the colliding protein. This loss of hydration also acts as a repulsive effect. Both of these repulsive effects are larger for larger proteins, making the activation energy for adsorption of the larger protein bigger. This was confirmed by calculations done by Jeon and Andrade.[67] A recent alternative model of the protein adsorption process, which focuses on the spatial arrangement of the PEG chains, arrives at similar conclusions with respect to the dependence of the adsorption rate on the protein size.[69]

Finally, Weaver and Pitt have tabulated sticking probabilities for a number of different proteins on various surfaces.[70] Values beween 10^{-8} and 10^{-5} have been observed. While the sticking probabilities obtained here for PhB and βGal fall within this range, the value for BSA is somewhat larger (Table 3). This descrepancy undoubtedly results from the approximate nature of a number of the experimental parameters that go into the calculation of the sticking probability in our experiment. For example, we have only approximate values for the length and surface area of the detection zone, the concentration of the protein in this zone, and the electrophoretic transport time through this zone.

Conclusions

We have investigated the effect of protein size and nanotube tip diameter on the resistive-pulse signature associated with electrophoretic translocation of protein analytes through conical nanotube sensors. We have found that the duration of the current-pulses associated with such translocation events are many orders of magnitude longer than the electrophoretic transport time of the protein through the nanotube detection zone. We have proposed a simple model that accounts for this key observation. This model assumes that the protein molecule engages in repeated adsorption/desorption events to/from the nanotube walls as it translocates through the detection zone.

(85) Reger, D. L., Goode, S. R., Mercer, E. E., Eds. *Chemistry, Principles and Practice*, 2nd ed.; Saunders: Orlando, 1997; p 550.
(86) Pauling, L. *General Chemistry*, 3rd ed.; Courier Dover Publications: New York, 1988; p 551.
(87) Bronshtein, I. N.; Semendyayev, K. A.; Musiol, G.; Muehlig, H.; Muehlig, H. *Handbook of Mathematics*, 4th ed.; Springer: New York, NY, 2004; eq 16.84.
(88) Skoog, D. A.; Holler, F. J.; Nieman, T. A. *Principles of Instrumental Analysis*, 5th ed.; Harcourt Brace College Publishers: Orlando, 1998; 829 pp.
(89) Prime, K. L.; Whitesides, G. M. *J. Am. Chem. Soc.* **1993**, *115*, 10714–10721.

This model not only accounts for the long pulse duration but also for the triangular shape of the current pulse (Figure 3) and the increase in the standard deviation of the pulse duration with increasing protein size (Table 1). While, in principle, the current-pulse should show current steps due to the individual protein-adsorption events,[82] the signal-to-noise ratio during the pulse is not sufficient to observe these steps. Figure 3C provides a good illustration of the noise level during a pulse. The results of our analyses are in general agreement with results obtained from other investigations of protein adsorption to surfaces.[65−70] This includes the observations that smaller proteins stick more readily to the surface but remain adsorbed for shorter times than larger proteins.[65−69] In addition, the sticking probabilities reported here are in general agreement with results obtained from other methods.[70]

The two key experimental parameters obtained from the resistive-pulse method are the pulse duration, τ, and the pulse amplitude, Δi. Our data show that pulse duration is a more useful metric for exploring the effect of protein size on current-pulse signature. This is because pulse duration varies more dramatically with protein size than does pulse amplitude. Indeed, within experimental error, the pulse amplitudes for the different proteins studied here are indistinguishable (Figure 4). We have recently developed an antibody-based method for resistive-pulse detection of specific protein molecules that takes advantage of the effect of protein-analyte size on pulse duration.[27]

Acknowledgment. This work was supported by the "Center of Excellence - Center for Nano-Biosensors" from the State University System of Florida, "Integrative Approaches to discover pathogenesis-associated proteins from the causal agency of citrus greening" from The Florida Citrus Advanced Technology Program, and the Army Research Office. L.T.S. also acknowledges the fellowship support from the ACS Division of Analytical Chemistry.

Supporting Information Available: Additional experimental procedures and possible scenarios to explain the current pulse data. This material is available free of charge via the Internet at http://pubs.acs.org.

JA100693X